frontiers in Physics

PERSPECTIVE
published: 03 March 2022
doi: 10.3389/fphy.2022.834658

Infinite-Layer Nickelate Superconductors: A Current Experimental Perspective of the Crystal and Electronic Structures

L. E. Chow and A. Ariando *

Department of Physics, Faculty of Science, National University of Singapore, Singapore

After the reward of more than 2 decades of pursuit on the high-T_c cuprate analog with the hope to obtain a better understanding of the mechanism of high-T_c superconductivity, the discovery of superconductivity in the infinite-layer nickelate brings more mystery to the picture than expected. Tops in the list of questions are perhaps 1) absence of superconductivity in the bulk nickelate and limited thickness of the infinite-layer phase in thin film, 2) absence of superconductivity in the La-nickelate despite it being the earliest studied rare-earth nickelate, and the role of 4 *f* orbital in the recipe of superconductivity, 3) absence of Meissner effect and suspect of the origin of superconductivity from the interface, 4) whether nickelate hosts similar pairing symmetry to the single-band high-T_c cuprates or multiband iron-based superconductor. In this perspective article, we will discuss the following aspects: 1) stabilization of the infinite-layer phase on the $SrTiO_3$(001) substrate and the thickness dependency of observables; 2) rare-earth dependence of the superconducting dome and phase diagram of the (La/Pr/Nd)- infinite-layer nickelate thin film; 3) experimental aspects of the measurement of Meissner effect; 4) theoretical framework and experimental study of the pairing symmetry of infinite-layer nickelate superconductor.

Keywords: infinite-layer nickelates, nickelate superconductivity, pairing symmetry, meissner effect, lanthanide nickelate, thickness dependence, rare earth magnetism

OPEN ACCESS

Edited by:
Junjie Zhang,
Shandong University, China

Reviewed by:
Xingjiang Zhou,
Institute of Physics (CAS), China

***Correspondence:**
A. Ariando
ariando@nus.edu.sg

Specialty section:
This article was submitted to Condensed Matter Physics, a section of the journal Frontiers in Physics

Received: *13 December 2021*
Accepted: *10 January 2022*
Published: *03 March 2022*

Citation:
Chow LE and Ariando A (2022) Infinite-Layer Nickelate Superconductors: A Current Experimental Perspective of the Crystal and Electronic Structures. Front. Phys. 10:834658. doi: 10.3389/fphy.2022.834658

MAIN TEXT

Around 4 decades ago, the witness of superconductivity above 30 K redefined preexisting knowledge on the mechanism of superconductivity and restructured the landscape of the playground on superconductor materials [1, 2]. Understanding the high-temperature (high-T_c) superconductivity has since been one of the holy grails in physics. Several characteristic properties were discussed in the cuprate superconductor: 1) quasi-2D CuO_2 square-planar lattice, 2) antiferromagnetic order and superexchange interaction, 3) spin $S = \frac{1}{2}$ half-filling state, 4) Cu^{2+} of 3 d^9 electronic configurations [3–7]. To identify which parameters are the key ingredients which drive the high-T_c superconductivity in cuprate, searching for isostructural compounds with some of these properties and comparing them to the cuprate were motivated [8]. Among all the cuprate analogs [9], nickelate of Ni^{1+} with the same 3 d^9 electronic configurations was identified as the closest cousin to the cuprate [7, 10]. For decades, theoretical and experimental efforts have been made to explore the lead [11–13]. Unlike cuprate, which was first synthesized in the bulk form, superconducting nickelate was only realized recently in the thin-film form [14–21], with Ni^{1+} in the

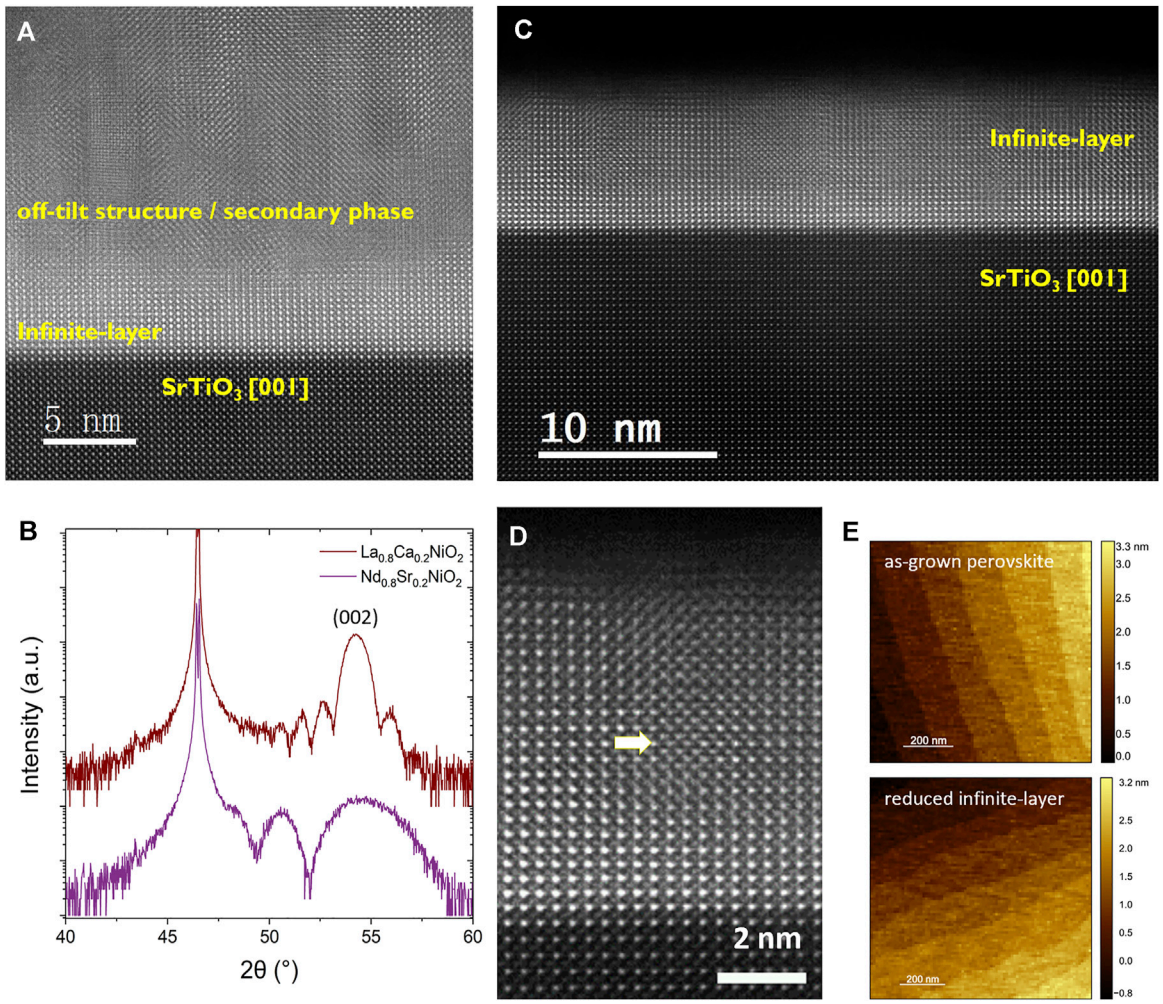

FIGURE 1 | Structural properties of the reduced infinite-layer nickelate thin film. **(A,C,D)** STEM HAADF images. **(B)** XRD (002) pattern. **(A)** A thick 30 nm $Nd_{0.85}Sr_{0.15}NiO_2$ film has infinite-layer phase stabilized up to ~5 nm from the substrate interface. Above 5 nm, secondary phase or off-tilt structure can be seen, data is adapted from [26]. Entire $Nd_{0.8}Sr_{0.2}NiO_2$ film of thinner <10 nm can be reduced to infinite-layer phase with perfect crystallinity **(C,D)** up to the surface, with no sign of secondary phase except for possible RP stacking fault occurs at some part of the film **(D)**. **(B)** A clear Laue fringes can be observed for 8 nm $Nd_{0.8}Sr_{0.2}NiO_2$ and 15 nm $La_{0.8}Ca_{0.2}NiO_2$ thin films, indicating coherent infinite-layer phase. **(E)** Atomic-force-microscopy (AFM) images show the atomically flat terrace-like surface topography in $Nd_{0.8}Sr_{0.2}NiO_2$ (6.5 nm) film surfaces before (top) and after (bottom) topotactic reduction done in the PLD chamber.

infinite-layer phase that can be achieved through topotactic reduction from the perovskite compound. Missing superconductivity in the bulk nickelate [22, 23] and limitation in stabilizing the infinite-layer phase above ~10 nm from the substrate [24–26] demands answers on the thickness-dependent crystallinity and electronic structure of the infinite-layer nickelate film. While lanthanide-cuprate La-Ba-Cu-O was the first superconducting compound synthesized [27], lanthanide-nickelate was initially reported to not host superconductivity, but superconductivity was only realized in the neodymium-based counterpart, a rare-earth element with 4 f magnetism [14]. The possible roles of rare-earth magnetism in the early observation of nickelate's superconductivity added layers of mystery to the newfound sister of cuprate [6, 28, 29]. In addition to the bulk nickelate not being reported to show superconductivity, concrete evidence of the Meissner effect in the superconducting nickelate thin film was missing [14], leading to the suspect whether the phenomenon was interfacial in nature. High-T_c cuprate is uniquely identified with a dominant $d_{x^2-y^2}$-wave gap which is believed to be mediated by the antiferromagnetic superexchange interaction, that poses as a crucial factor in the high-T_c superconductivity [3]. Hence, answering the superconducting order parameter in the nickelate is the top priority. However, the challenge in the fabrication of high-quality infinite-layer nickelate films obstructed the experimental means to investigate, especially with those surface-sensitive techniques are not applicable when bad crystallinity or secondary phases are prone to form at the surface of nickelate superconducting thin-film [25]. Overall, while the discovery of superconductivity in the nickelate provided an exciting playground to study the highly correlated system, the newfound superconductor family also ignited controversial debates that will reshape high-T_c

framework [4–6, 30–37]. In this article, we provided a contemporary experimental perspective on the topics.

THICKNESS DEPENDENCE

Stabilization of Infinite-Layer Phase

Since the observation of superconductivity in the infinite-layer nickelate $Nd_{0.8}Sr_{0.2}NiO_2$ thin film [14], apparent challenges have emerged in material synthesis [25]. On top of low reproducibility and difficulty in the fabrication of superconducting doped infinite-layer structure by many experimental groups [38, 39], a hard-nut-to-crack issue is a limited thickness from the substrate interface, which the infinite-layer phase can be stabilized [25, 26, 40]. Above ~10 nm from the substrate interface, obvious secondary phases or off-tilt structures form instead of the infinite-layer or partially reduced perovskite phase [25]. In many cases, growing a thick film will lead to the formation of a secondary phase even at just ~5 nm from the substrate (**Figure 1A**) [26]. On the other hand, if a thinner <10 nm film is grown, the entire film can be fully reduced with no observation of secondary phase even at the film surface (**Figures 1C,D**), except for possibly Ruddlesden-Popper (RP) stacking fault at some regions of the film (**Figure 1D**). The obvious strategy for obtaining the purest possible infinite-layer phase is fabricating thin films below 10 nm. In addition to the absence of secondary phases as shown in the STEM image, atomically flat surfaces with terrace-like topography can be observed on the film surface before and after topotactic reduction, as shown in the atomic-force-microscopy images in **Figure 1E**. Some reports suggested using $SrTiO_3$ (STO) capping layer on top of the nickelate thin film prior to a topotactic reduction that can serve as a "backbone" to help stabilize the infinite-layer phase during topotactic reduction from the perovskite phase [25, 41]. However, such a method has not led to a thicker infinite-layer phase of >10 nm. Lattice coherency of a crystalline thin film can be seen from the X-ray diffraction (XRD) Laue fringes which originate from the constructive interference between perfect lattice layers of the thin film. To date, most reported XRD data of the perovskite phase of the doped nickelate thin film has clear Laue fringes in the vicinity of the (002) peak; however, Laue fringes are typically absent for the reduced doped infinite-layer nickelate (002) peak [16, 26, 41–43]. This may suggest the presence of nonstoichiometric oxygen at random parts of the reduced infinite-layer thin film. Significant development of secondary or perovskite phases is typically avoided after optimization in film growth conditions since no perovskite peak or defect phase peak is seen in the XRD curve.

The challenge of obtaining a coherent infinite-layer phase does not affect transport-related study since zero resistance can be observed even when only a small part of the film is superconducting. Unfortunately, the same cannot be said for measurements requiring a pure phase with coherent crystallinity, especially at the film surface, such as the Angle-resolved Photoemission Spectroscopy (ARPES) or Scanning Tunneling Spectroscopy (STS). Many probing techniques which reveal crucial aspects of the superconductivity in nickelate cannot be carried out because of the lack of coherent lattice and purity in the infinite-layer phase, especially on the top surface. With much effort in optimizing film quality, we recently reported an observation of clear Laue fringes in the vicinity of XRD (002) peak of the infinite-layer phase for $Nd_{1-x}Sr_xNiO_2$ and $La_{1-x}Ca_xNiO_2$ (**Figure 1B**). Especially in the case of superconducting lanthanide infinite-layer nickelate, more than 30 unit-cells (uc) of a coherent infinite-layer lattice can be seen vividly from the XRD Laue fringes.

Thickness Dependency and Role of Strain and Interface

Superconductivity is missing in the bulk infinite-layer nickelate [23, 44–46]. The puzzling limitation in the thickness of the infinite-layer thin film further warrants the importance of investigating the thickness dependency of the physical observables and electronic structure of the infinite-layer nickelate. The zero-resistivity critical temperature , $T_{c,0}$, of $Pr_{0.8}Sr_{0.2}NiO_2$ thin film with thickness from 5.3 to 12 nm has been reported [8], showing a slight decrease from 5.3 to 8 nm and it then increases again up to 12 nm. However, the normal state resistivity of the same samples also shows corresponding change, where high $T_{c,0}$ samples have low resistivity. This implies the stronger correlation between $T_{c,0}$ and normal state resistivity but not the film thickness [25]. On the other hand, the $T_{c,0}$ of $Nd_{0.8}Sr_{0.2}NiO_2$ thin films monotonically increases with film thickness (4.6–10.1 nm) observed from both resistivity and susceptibility measurements [24]. In addition, a systematic evaluation of the thickness-dependent electronic structure has been shown with the change in Hall coefficients and XAS spectra of $Nd_{0.8}Sr_{0.2}NiO_2$ thin film from 4.6 to 10.1 nm [24]. The results imply strain modulation and interface effect in the infinite-layer nickelate.

RARE-EARTH DEPENDENCE

Doping Dependent Phase Diagram

The barium (Ba) hole-doped lanthanide La-cuprate $La_{2-x}Ba_xCuO_4$ was the first high-T_c cuprate synthesized, which kicked off the door to high-temperature superconductivity beyond the BCS paradigm [27]. To mimic cuprate's square-planar structure and 3 d^9 electronic configurations, Ni^{1+} state in nickelate was predicted to be an ideal cuprate analog to assist in the understanding of the origin of high-T_c superconductivity in cuprate [4, 7, 13, 14, 34, 47, 48]. Naturally, lanthanum (La) was the first rare-earth option to be looked for in nickelate. Many experimental attempts were made on La-nickelate to achieve superconductivity with Ni^{1+} state in the form of superlattices, infinite-layer structure for the past 2 decades [12, 14, 49, 50]. Despite the long search, La-nickelate was initially found not to be superconducting and the first observation of nickelate superconductivity was realized by Sr-doped on a smaller neodymium ion Nd-infinite-layer nickelate thin film with 4f magnetism in 2019 [14]. Since then, superconductivity in the infinite-layer nickelate family has been quickly expanded to another neighbor with rare-earth magnetism in the rare-earth series, praseodymium (Pr) [42], and has been successfully reproduced by multiple experimental groups [17, 51]. However, superconductivity in La-nickelate, which has an empty 4f orbital, still seems non-existent for another 2 years until it was successfully realized independently by two different groups in the Ca-doped La_{1-}

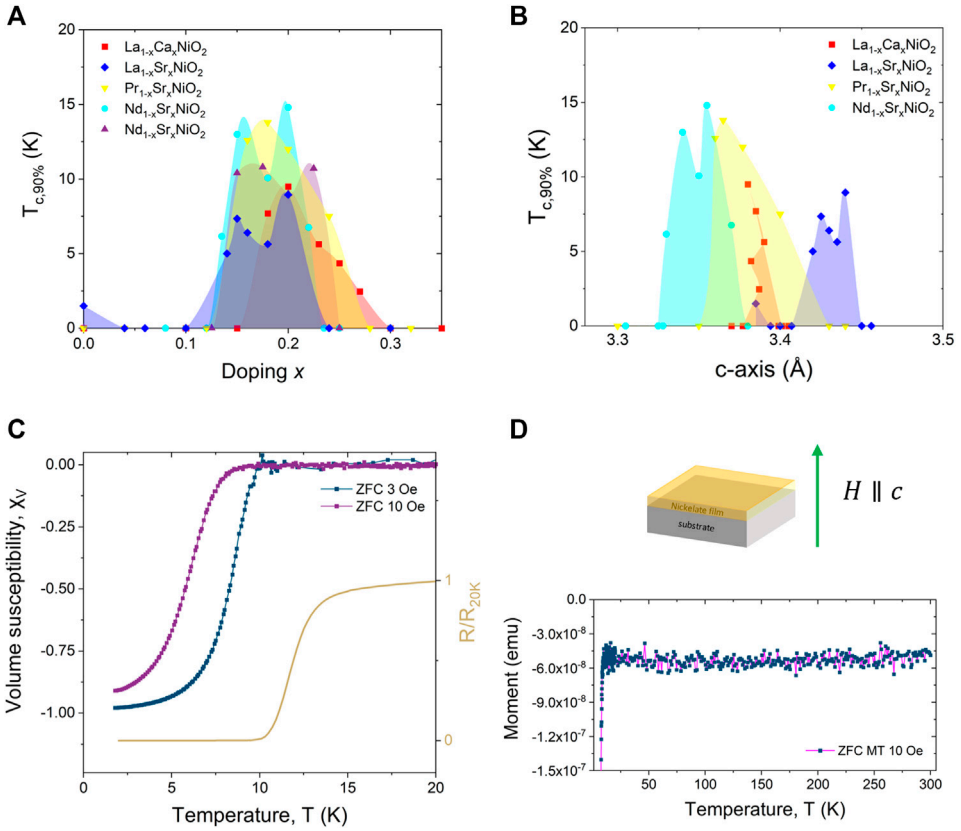

FIGURE 2 | (A,B) Superconducting phase diagram of various hole doped infinite-layer nickelates, plotted as a function of hole doping levels *x* **(A)** and c-axis lattice constant **(B)**. Data are adapted from (La, Ca) [16], (La,Sr) [41], (Pr, Sr) [15], (Nd, Sr) [26, 40]. **(C,D)** Observation of Meissner effect in the superconducting infinite-layer thin film at $H \parallel c$. Superconducting transition observed in resistivity and susceptibility **(C)** measurements for $Nd_{0.8}Sr_{0.2}NiO_2$ thin film. **(D)** The measured moment at above T_c is typically of -10^{-8} emu scale and almost constant at $T_{c,onset} < T < 300K$, correspond to STO substrate diamagnetic signal.

$_xCa_xNiO_2$ [16] and Sr-doped $La_{1-x}Sr_xNiO_2$ [41] infinite-layer thin film. Given the missing report of superconductivity in La-nickelate for almost 2 decades, the role of 4 *f* magnetism and other differences between $LaNiO_2$ and (Pr/Nd)NiO_2 in the recipe of superconductivity become an open question and inspire further investigation on their pairing symmetries, anisotropy and doping dependent phase diagram [16, 26, 28, 29, 40, 41, 52–55].

Figure 2A shows doping-dependent superconducting dome and phase diagram in various Sr-doped and Ca-doped rare-earth (La, Pr, Nd) infinite-layer nickelate synthesized so far [15, 16, 26, 40, 41]. The first eye-catching feature is the presence of "dip" with a lower T_c for a particular doping in the $Nd_{1-x}Sr_xNiO_2$ [26, 40] and $La_{1-x}Sr_xNiO_2$ [41] thin films. Given the lack of consistency of the "dip" feature on a particular doping across different rare-earth nickelates and reports, it is presently unclear whether it is an experimental artifact or a reminiscence of certain quantum critical transitions in the system. The second observation is the expansion of the superconducting dome to a higher doping level from $Nd_{1-x}Sr_xNiO_2$, $Pr_{1-x}Sr_xNiO_2$ to $La_{1-x}Ca_xNiO_2$. Given the increased difficulty in synthesizing infinite-layer nickelate thin film at larger doping [25, 41], such observation may have a certain correlation to film crystallinity. The perovskite nickelate has a smaller in-plane lattice constant than the $SrTiO_3$ (001) substrate, which the lattice mismatches are decreasing from $NdNiO_3$ to $LaNiO_3$. It has been established that a perovskite phase nickelate with good crystallinity is essential to the success in topotactic reduction to the infinite-layer phase [25]. One may suggest that perovskite $La_{1-x}Ca_xNiO_3$ and $Pr_{1-x}Sr_xNiO_3$ can be grown to have better crystallinity than the $Nd_{1-x}Sr_xNiO_3$ at a large doping regime. A similar argument could be made for the difference in superconducting dome between $La_{1-x}Ca_xNiO_2$ and $La_{1-x}Sr_xNiO_2$. The Ca^{2+} ion is of more similar size to the rare-earth La^{3+}, Pr^{3+} and Nd^{3+} ions than the larger Sr^{2+} ion [16]. Regardless, it is also possible that different rare-earth ion and cation doping leads to a slight difference in the electronic band structure of the infinite-layer nickelate, causing a different span of superconducting domes. Another note is, so far, the doping level in the fabricated thin films is expected to follow the stoichiometry of the polycrystalline target used in the pulsed-laser-deposition (PLD) growth. It is not warranted that the doping level is accurate, and further investigation on the stoichiometry of the doped thin film shall be carried out. The third observation is the correlation between the size of the rare-earth ions and superconducting transition temperature T_c. The maximum

onset temperature in resistivity, where resistivity reaches 90% of its value at 20 K, $T_{c,90\%}$ is roughly consistent among various reports, where La-nickelate has $T_{c,90\%}$ ~9–10 K while Pr- and Nd-nickelate has $T_{c,90\%}$ ~12–15 K. It is routinely explained by the increase in electronic bandwidth for a smaller rare-earth ion [14, 16].

In addition to the difference in the superconducting T_c between La- and (Pr/Nd)- infinite-layer nickelate, the Hall coefficient (R_H) sign change temperature across doping levels also exhibits dissimilarity between La- and (Pr/Nd)-nickelate. R_H sign change temperature is monotonically increasing with hole doping in the case of (Pr/Nd)- infinite-layer nickelate [15, 26, 40], which may suggest increased-dominancy in $d_{x^2-y^2}$ hole pocket at Fermi level with increasing hole doping. However, in the case of $La_{1-x}Ca_xNiO_2$, the R_H sign change temperatures are constant at around 35 K between $0.23 \leq x \leq 0.3$ and the difference in R_H at low temperature is small at increasing doping [16]. While preliminary and possibly confounded by the impact of in-plane compressive stress from the substrate, the role of hole doping is likely to be different in modifying the band structure of the Ca-doped La-nickelate as compared to the Sr-doped (Pr/Nd)-nickelate.

Relevance to Lattice Constant

Since superconductivity has not been observed in the bulk infinite-layer nickelate despite that high crystallinity samples were made [44, 45], the ab-axis lattice constants of the superconducting infinite-layer thin film are epitaxially constrained to the substrate in-plane lattice constants. It might be intuitive to look for any correlation between the c-axis lattice dimension and superconducting dome of the infinite-layer nickelate (**Figure 2B**). At first glance, the superconducting dome is generally limited to between 3.32 Å and 3.45 Å. However, the superconducting domes between various rare-earth compounds do not completely overlap. Also, for the case of $La_{1-x}Ca_xNiO_2$, the variation in c-axis lattice constant across doping is small due to a very similar ionic size between Ca^{2+} ion and La^{3+}, and has slight sample-to-sample variation at the same Ca doping [16]. It seems early to suggest any strict correlation between the superconducting dome of infinite-layer nickelate and the c-axis lattice dimension. It is worth noting that an enhancement in onset T_c was realized experimentally by applying external pressure [17], which suggests the likelihood of further increasing T_c by simulating chemical pressure through tuning in-plane lattice constants, rare-earth ions size, or dopant size. In addition, we note that there are recent theoretical calculations on the effect of in-plane lattice constant and epitaxial strain in tuning the *P4/mmm - I4/mcm* phase transition in $RNiO_2$ (R = La, Pr, Nd, Eu-Lu, Y) [56, 57].

OBSERVATION OF MEISSNER EFFECT

Two main phenomena characterize superconductivity: 1) zero electrical resistivity, 2) Meissner effect. The first experimental report of the discovery of superconductivity in $Nd_{0.8}Sr_{0.2}NiO_2$ thin film provided multiple resistivity-temperature ($R-T$) curves with clear zero resistivity data and two-coil mutual inductance measurement to observe the expulsion of the magnetic field in the Meissner state [14]. However, the real part of the pickup voltage $Re(V_p)$ does not go to zero as expected for a superconductor in the Meissner state. Some diamagnetic signal is observed, but the $Re(V_p)$ measured the lowest temperature is far from zero as compared to the change within the transition $Re(V_p) \sim 1.7 \rightarrow 1.25\,\mu V$ [14]. The absence of concrete data to support the presence of Meissner state led to a suspicion that the superconductivity in nickelate arises from the interface with the substrate but is not intrinsic to the bulk material.

Meissner effect is routinely seen in the magnetic susceptibility measurement: 1) a negative slope in the $M-H$ curve which ends at the lower critical field H_{c1}, 2) negative diamagnetic signal below T_c in $M-T$ curve which the volume susceptibility χ_V (in S. I. unit) goes to -1 for Meissner state. The $M-T$ and $M-H$ data were not presented in the early reports of the superconductivity observed in the infinite-layer nickelate thin films. Zeng *et al.* provided a study on the thickness-dependent effect on the film's T_c in both resistivity and susceptibility measurements [24]. The diamagnetic moment in $M-T$ curve (measured at $H \parallel c$) below the superconducting transition is typically of ~ 10^{-5} emu scale for a $2.5 \times 5\,mm^2$ superconducting thin film of 8 nm thick. After demagnetizing field correction, the volume susceptibility at 2 K can be calculated to be $\chi_V < -0.9$ which is fairly close to -1 for perfect diamagnetism (**Figure 2C**). **Figure 2D** presents the raw data for the magnetic moment measured above transition $T > T_{c,onset}$. The infinite-layer thin film on STO substrate has an almost temperature-independent moment for $T_{c,onset} < T < 300K$, which the small ~ 10^{-8} emu negative moment measured shall correspond to the STO substrate diamagnetic signal. In addition, a negative slope in $M-H$ curve was also observed in superconducting $Nd_{0.8}Sr_{0.2}NiO_2$ thin film, resembling the Meissner effect and bulk superconductivity, which is intrinsic to the nickelate thin film but not of the interface. The lower critical field H_{c1} is defined as the magnetic field in the sample which the field penetrates the sample volume and the onset of mixed state for type II superconductor. In the $M-H$ curve, due to the thin-film nature with large demagnetizing factor $N \rightarrow 1$ for $H \parallel c$, the $H_{c1}^{applied}$ before demagnetization factor correction is around and less than 1Oe, which is difficult to be resolved and has a large error in the calculation of actual H_{c1}. After demagnetizing factor correction, the $H_{c1}\,(T = 0K)$ is approximated to be around 79 Oe.

The superconducting transition temperature observed in the $M-T$ curve typically has an onset close to the $T_{c,0}$ in resistivity provided good homogeneity of the entire sample (**Figure 2C**). Lower $T_{c,\,onset}$ in $M-T$ can be measured if the applied field is larger than the lower critical field $H > H_{c1}$. Since the applied $H_{c1}^{applied} \leq 1$ Oe for $Nd_{0.8}Sr_{0.2}NiO_2$ infinite-layer nickelate thin film, a larger measuring field of 10 Oe can lead to lower $T_{c,\,onset}$ and smaller $\chi_V\,(2K)$ as compared to 3 Oe measuring field, for example. In addition, the Meissner effect will not be observable, or only a very small diamagnetic signal is observed if there are inhomogeneity and defect phases in the infinite-layer

nickelate thin film, which can easily present even when a high T_c is observed in the resistivity $R-T$ data.

PAIRING SYMMETRY

Dominant *d*-wave Gap

The infinite-layer nickelate is a sister of the high-T_c cuprate, which hosts a dominant $d_{x^2-y^2}$-wave gap, both sharing a similar crystal structure and 3 d^9 electronic configuration. In the recent resonant inelastic X-ray scattering (RIXS) experiments at Ni L_3-edge on the infinite-layer nickelate thin films, charge order and spin wave of antiferromagnetically coupled spins in a square lattice was observed [43, 58–60]. The antiferromagnetic exchange coupling strength J is estimated to be around 63.6 meV in RIXS. While a different J value can be estimated with different spin model calculation, the general consensus is that the nickelate's J value is smaller than the $J \sim 130$ **meV** of the high-T_c cuprates [58, 61]. In addition, exchange bias effect was observed at a ferromagnet/$Nd_{0.8}Sr_{0.2}NiO_2$(20 nm) interface which could be interpreted as the antiferromagnetic nature at the surface of thick $Nd_{0.8}Sr_{0.2}NiO_2$ film (though exchange bias field is absent for $\leq$ 10 nm film) [18]. Despite the lack of concrete proof on the long-range magnetic order to date, the $t-J$ model used in cuprates is perceived to be suitable to capture nickelate's superconductivity [55] and the general consensus across different theoretical calculations on the superconducting pairing symmetry of nickelate is a dominant $d_{x^2-y^2}$-wave pairing like the cuprate with some pointed out various possibility of multiband superconductivity [35, 52, 55, 62]. In the $t-J-K$ model which accounted for the Kondo coupling in nickelate, an interstitial s-wave gap exists at the large hole doping and small t/K region of the phase diagram [63]. On the other hand, if hopping t/K is large as compared to the Kondo coupling, a dominant d-wave pairing or a transition from $(d+is)$-wave at low doping to d-wave at large doping is expected [63].

Considering the role of nickelate superconductivity in illuminating the origin of high-T_c superconductivity in cuprates, a detailed experimental study on the pairing symmetry of nickelate is crucial. The first experimental report on the superconducting gap symmetry of the infinite-layer nickelate is a single-particle-tunneling experiment on $Nd_{0.8}Sr_{0.2}NiO_2$ film surface which detected signals correspond to s-wave, d-wave or a mixture of both in different parts of the film surface [19]. However, we note here the difficulty in achieving a good crystallinity and high purity of the superconducting phase, especially near the film surface of the reduced infinite-layer thin film. Hence, surface-sensitive techniques which are useful in determining the gap profile like the angle-resolved photoemission spectroscopy (ARPES) may not be feasible to investigate the pairing order of the infinite-layer nickelate thin films until the film quality at the surface is perfected. Furthermore, phase-sensitive experiments are also waiting to be seen [64].

Fully Gapped Pairing and Isotropic Upper Critical Field

While the tunneling experiment did not lead to a complete answer of the nickelate's pairing order, the existence of a fully gapped s-wave signal ignited multiple explanations to the observation [63, 65]. Recently the upper critical field H_{c2} of $Nd_{0.775}Sr_{0.225}NiO_2$ thin film is measured to be mostly isotropic down to the lowest temperature and is smaller than the Pauli limit [66]. The isotropic H_{c2} in the $Nd_{0.775}Sr_{0.225}NiO_2$ infinite-layer nickelate is completely distinct from the cuprate with large anisotropy and other quasi-2D superconductors. On the other hand, this isotropic upper critical field behavior places nickelate to be more similar to the high-T_c multiband iron-based superconductor which is believed to host nodeless $s_{\pm}$-wave multigap pairing [67, 68]. Further investigation on the nickelate's controversial pairing symmetry is warranted [69, 70].

DATA AVAILABILITY STATEMENT

The original contributions presented in the study are included in the article/Supplementary Material, further inquiries can be directed to the corresponding author.

AUTHOR CONTRIBUTIONS

All authors listed have made a substantial, direct, and intellectual contribution to the work and approved it for publication.

FUNDING

This research is supported by the Agency for Science, Technology, and Research (A*STAR) under its Advanced Manufacturing and Engineering (AME) Individual Research Grant (IRG) (A1983c0034) and the Singapore National Research Foundation (NRF) under the Competitive Research Programs (CRP Grant No. NRF-CRP15-2015-01) and by the Ministry of Education, Singapore, under its MOE Tier 2 grant (Grant no. MOE-T2EP50121-0018).

ACKNOWLEDGMENTS

We thank S. W. Zeng for the fruitful discussion and revision of this article. We acknowledge Elbert E. M. Chia, C. Z. Diao, W. Escoffier, M. Goiran, S. K. Goh, J. X. Hu, H. Jani, Z. S. Lim, C. J. Li, P. Nandi, G. J. Omar, M. Pierre, D. Preziosi, S. K. Sudheesh, M. Salluzzo, C. S. Tang, Andrew T. S. Wee, K. Y. Yip, X. M. Yin, P. Yang, Z. T. Zhang for discussions.

REFERENCES

1. Wu MK, Ashburn JR, Torng CJ, Hor PH, Meng RL, Gao L, et al. Superconductivity at 93 K in a New Mixed-phase Y-Ba-Cu-O Compound System at Ambient Pressure. *Phys Rev Lett* (1987) 58:908–10. doi:10.1103/physrevlett.58.908
2. Azuma M, Hiroi Z, Takano M, Bando Y, Takeda Y. Superconductivity at 110 K in the Infinite-Layer Compound (Sr1-xCax)1-yCuO2. *Nature* (1992) 356:775–6. doi:10.1038/356775a0
3. Keimer B, Kivelson SA, Norman MR, Uchida S, Zaanen J. From Quantum Matter to High-Temperature Superconductivity in Copper Oxides. *Nature* (2015) 518:179–86. doi:10.1038/nature14165
4. Botana AS, Bernardini F, Cano A. Nickelate Superconductors: An Ongoing Dialog between Theory and Experiments. *J Exp Theor Phys* (2021) 132:618–27. doi:10.1134/s1063776121040026
5. Jiang M, Berciu M, Sawatzky GA. Critical Nature of the Ni Spin State in Doped NdNiO2. *Phys Rev Lett* (2020) 124:207004. doi:10.1103/physrevlett.124.207004
6. Pickett WE. The Dawn of the Nickel Age of Superconductivity. *Nat Rev Phys* (2021) 3:7–8. doi:10.1038/s42254-020-00257-3
7. Botana AS, Norman MR. Similarities and Differences between LaNiO2 and CaCuO2 and Implications for Superconductivity. *Phys Rev X* (2020) 10:011024. doi:10.1103/physrevx.10.011024
8. Rice TM. Electronic Structure of Possible Nickelate Analogs to the Cuprates. *Phys Rev B - Condens Matter Mater Phys* (1999) 59:7901.
9. Maeno Y, Hashimoto H, Yoshida K, Nishizaki S, Fujita T, Bednorz JG, et al. Superconductivity in a Layered Perovskite without Copper. *Nature* (1994) 372:532–4. doi:10.1038/372532a0
10. Bernardini F, Olevano V, Blase X, Cano A. Infinite-Layer Fluoro-Nickelates as D9 Model Materials. *J Phys Mater* (2020) 3:035003. doi:10.1088/2515-7639/ab885d
11. Lee KW, Pickett WE. Infinite-Layer LaNiO2: Ni1+ Is Not Cu2+ [33]. *Phys Rev B - Condens Matter Mater Phys* (2004) 70:1. doi:10.1103/physrevb.70.165109
12. Chaloupka J, Khaliullin G. Orbital Order and Possible Superconductivity in LaNiO3/LaMO3 Superlattices. *Phys Rev Lett* (2008) 100:016404. doi:10.1103/PhysRevLett.100.016404
13. Zhang J, Botana AS, Freeland JW, Phelan D, Zheng H, Pardo V, et al. Large Orbital Polarization in a Metallic Square-Planar Nickelate. *Nat Phys* (2017) 13:864–9. doi:10.1038/nphys4149
14. Li D, Lee K, Wang BY, Osada M, Crossley S, Lee HR, et al. Superconductivity in an Infinite-Layer Nickelate. *Nature* (2019) 572:624–7. doi:10.1038/s41586-019-1496-5
15. Osada M, Wang BY, Lee K, Li D, Hwang HY. Phase Diagram of Infinite Layer Praseodymium Nickelate Pr1-XSrxNiO2 Thin Films. *Phys Rev Mater* (2020) 4:1. doi:10.1103/physrevmaterials.4.121801
16. Zeng SW, Li CJ, Chow LE, Cao Y, Zhang ZT, Tang CS, et al. Superconductivity in Infinite-Layer Lanthanide Nickelates. *Sci Adv* (2022) 8:eabl9927. doi:10.1126/sciadv.abl9927
17. Wang NN, Yang MW, Chen KY, Yang Z, Zhang H, Zhu ZH, et al. Pressure-Induced Monotonic Enhancement of Tc to over 30 K in the Superconducting Pr0.82Sr0.18NiO2 Thin Films. *arXiv* [Preprint] (2021). Available from: https://arXiv.org/abs/2109.12811.
18. Zhou X, Zhang X, Yi J, Qin P, Feng Z, Jiang P, et al. Antiferromagnetism in Ni-Based Superconductors. *Adv Mater* (2021) 34 2106117. doi:10.1002/adma.202106117
19. Gu Q, Li Y, Wan S, Li H, Guo W, Yang H, et al. Single Particle Tunneling Spectrum of Superconducting Nd1-XSrxNiO2 Thin Films. *Nat Commun* (2020) 11:6027. doi:10.1038/s41467-020-19908-1
20. Pan GA, Segedin DF, LaBollita H, Song Q, Nica EM, Goodge BH, et al. Superconductivity in a Quintuple-Layer Square-Planar Nickelate. *Nat Mater* (2022) 21:160–4. doi:10.1038/s41563-021-01142-9
21. Gao Q, Zhao Y, Zhou XJ, Zhu Z. Preparation of Superconducting Thin Films of Infinite-Layer Nickelate Nd0.8Sr0.2NiO2. *Chin Phys. Lett.* (2021) 38:5. doi:10.1088/0256-307x/38/7/077401
22. Cui Y, Li C, Li Q, Zhu X, Hu Z, Yang YF, et al. NMR Evidence of Antiferromagnetic Spin Fluctuations in Nd0.85Sr0.15NiO2. *Chin Phys. Lett.* (2021) 38. doi:10.1088/0256-307x/38/6/067401
23. Wang BX, Zheng H, Krivyakina E, Chmaissem O, Lopes PP, Lynn JW, et al. Synthesis and Characterization of Bulk Nd1-XSrxNi O2 and Nd1-XSrxNi O3. *Phys Rev Mater* (2020) 4:1. doi:10.1103/physrevmaterials.4.084409
24. Zeng SW, Yin XM, Li CJ, Tang CS, Han K, Huang Z, et al. Observation of Perfect Diamagnetism and Interfacial Effect on the Electronic Structures in Infinite Layer Nd0.8Sr0.2NiO2 Superconductors. *Nat Commun* (2022) 13:743. doi:10.1038/s41467-022-28390-w
25. Lee K, Goodge BH, Li D, Osada M, Wang BY, Cui Y, et al. Aspects of the Synthesis of Thin Film Superconducting Infinite-Layer Nickelates. *APL Mater* (2020) 8:041107. doi:10.1063/5.0005103
26. Zeng S, Tang CS, Yin X, Li C, Li M, Huang Z, et al. Phase Diagram and Superconducting Dome of Infinite-Layer Nd1−xSrxNiO2 Thin Films. *Phys Rev Lett* (2020) 125:147003. doi:10.1103/physrevlett.125.147003
27. Bednorz JG, Müller KA. Possible highT C Superconductivity in the Ba?La?Cu?O System. *Z Physik B - Condensed Matter* (1986) 64:189–93. doi:10.1007/bf01303701
28. Choi M-Y, Lee K-W, Pickett WE. Role of 4f States in Infinite-Layer NdNiO2. *Phys Rev B* (2020) 101:20503. doi:10.1103/physrevb.101.020503
29. Zhang R, Lane C, Singh B, Nokelainen J, Barbiellini B, Markiewicz RS, et al. Magnetic and F-Electron Effects in LaNiO2 and NdNiO2 Nickelates with Cuprate-like 3dx2−y2 Band. *Commun Phys* (2021) 4:1. doi:10.1038/s42005-021-00621-4
30. Norman MR. Entering the Nickel Age of Superconductivity. *Physics (College. Park. Md).* (2020) 13:1. doi:10.1103/physics.13.85
31. Zhang J, Tao X, Review on Quasi-2D Square Planar Nickelates, 23 (n.d.). (2021)
32. Kitatani M, Si L, Janson O, Arita R, Zhong Z, Held K. Nickelate Superconductors—A Renaissance of the One-Band Hubbard Model. *Npj Quan Mater* (2020) 5:6. doi:10.1038/s41535-020-00260-y
33. Liu Z, Xu C, Cao C, Zhu W, Wang ZF, Yang J. Doping Dependence of Electronic Structure of Infinite-Layer NdNiO2. *Phys Rev B* (2021) 103:1. doi:10.1103/physrevb.103.045103
34. Sawatzky GA. Superconductivity Seen in a Non-magnetic Nickel Oxide. *Nature* (2019) 572:592–3. doi:10.1038/d41586-019-02518-3
35. Zhang Y-H, Vishwanath A. Type-II T − J Model in Superconducting Nickelate Nd 1 − X Sr X NiO 2. *Phys Rev Res* (2020) 2:1. doi:10.1103/physrevresearch.2.023112
36. Botana AS, Lee K-W, Norman MR, Pardo V, Pickett WE. Low Valence Nickelates: Launching the Nickel Age of Superconductivity. *Front Phys* (2022) 9:813532. doi:10.3389/fphy.2021.813532
37. Nomura Y, Arita R. Superconductivity in Infinite-Layer Nickelates. *arXiv* [Preprint] (2021). Available from: https://arXiv.org/abs/2107.12923.
38. Si L, Xiao W, Kaufmann J, Tomczak JM, Lu Y, Zhong Z, et al. Topotactic Hydrogen in Nickelate Superconductors and Akin Infinite-Layer Oxides ABO_{2}. *Phys Rev Lett* (2020) 124:166402. doi:10.1103/PhysRevLett.124.166402
39. Li Y, Sun W, Yang J, Cai X, Guo W, Gu Z, et al. Impact of Cation Stoichiometry on the Crystalline Structure and Superconductivity in Nickelates. *Front Phys* (2021) 9:1. doi:10.3389/fphy.2021.719534
40. Li D, Wang BY, Lee K, Harvey SP, Osada M, Goodge BH, et al. Superconducting Dome in Nd 1- X Sr X NiO 2 Infinite Layer Films. *Phys Rev. Lett* (2020) 1.
41. Osada M, Wang BY, Goodge BH, Harvey SP, Lee K, Li D, et al. Nickelate Superconductivity without Rare-Earth Magnetism: (La,Sr)NiO2. *Adv Mater* (2021) 33:1. doi:10.1002/adma.202104083
42. Osada M, Wang BY, Goodge BH, Lee K, Yoon H, Sakuma K, et al. A Superconducting Praseodymium Nickelate with Infinite Layer Structure. *Nano Lett* (2020) 20:5735–40. doi:10.1021/acs.nanolett.0c01392
43. Tam CC, Choi J, Ding X, Agrestini S, Nag A, Huang B, et al. Charge Density Waves in Infinite-Layer NdNiO$_2$ Nickelates. *arXiv* [Preprint] (2021). Available from: https://arXiv.org/abs/2112.04440.
44. Li Q, He C, Si J, Zhu X, Zhang Y, Wen HH. Absence of Superconductivity in Bulk Nd1-XSrxNiO2. *Commun Mater* (2020) 1:16. doi:10.1038/s43246-020-0018-1
45. Puphal P, Wu Y, Fürsich K, Lee H, Pakdaman M, Bruin JAN, et al. Topotactic Transformation of Single Crystals : From Perovskite to Infinite-Layer Nickelates. *Sci Adv* (2021) 7:eabl8091. doi:10.1126/sciadv.abl8091
46. He C, Ming X, Li Q, Zhu X, Si J, Wen H-H. Synthesis and Physical Properties of Perovskite Sm1−x Sr X NiO3 (X = 0, 0.2) and Infinite-Layer Sm0.8Sr0.2NiO2

Nickelates. *J Phys Condens Matter* (2021) 33:265701. doi:10.1088/1361-648x/abfb90
47. Goodge BH, Li D, Lee K, Osada M, Wang BY, Sawatzky GA, et al. Doping Evolution of the Mott-Hubbard Landscape in Infinite-Layer Nickelates. *Proc Natl Acad Sci U S A* (2021) 118:1. doi:10.1073/pnas.2007683118
48. Miller C, Botana AS. Cupratelike Electronic and Magnetic Properties of Layered Transition-Metal Difluorides from First-Principles Calculations. *Phys Rev B*(2020) 101:195116. doi:10.1103/physrevb.101.195116
49. Takamatsu T, Kato M, Noji T, Koike Y. Low-Temperature Synthesis of the Infinite-Layer Compound LaNiO2 Using CaH2 as Reductant. *Phys C Supercond Its Appl* (2010) 470:2009. doi:10.1016/j.physc.2009.10.132
50. Ikeda A, Manabe T, Naito M. Improved Conductivity of Infinite-Layer LaNiO2 Thin Films by Metal Organic Decomposition. *Physica C: Superconductivity* (2013) 495:134–40. doi:10.1016/j.physc.2013.09.007
51. Ren X, Gao Q, Zhao Y, Luo H, Zhou X, Zhu Z. Superconductivity in Infinite-Layer Pr$_{0.8}$Sr$_{0.2}$NiO$_2$ Films on Different Substrates. *arXiv* [Preprint] (2021). Available from: https://arXiv.org/abs/2109.05761.
52. Adhikary P, Bandyopadhyay S, Das T, Dasgupta I, Saha-Dasgupta T. Orbital-Selective Superconductivity in a Two-Band Model of Infinite-Layer Nickelates. *Phys Rev B* (2020) 102:1. doi:10.1103/physrevb.102.100501
53. Hepting M, Li D, Jia CJ, Lu H, Paris E, Tseng Y, et al. Electronic Structure of the Parent Compound of Superconducting Infinite-Layer Nickelates. *Nat Mater* (2020) 19:381–5. doi:10.1038/s41563-019-0585-z
54. Jiang P, Si L, Liao Z, Zhong Z. Electronic Structure of Rare-Earth Infinite-Layer RNi O2(R=La,Nd). *Phys Rev B* (2019) 100:1. doi:10.1103/physrevb.100.201106
55. Wu X, Di Sante D, Schwemmer T, Hanke W, Hwang HY, Raghu S, et al. Robust Dx2-Y2-Wave Superconductivity of Infinite-Layer Nickelates. *Phys Rev B* (2020) 101:1. doi:10.1103/physrevb.101.060504
56. Bernardini F, Bosin A, Cano A. Geometric Effects in the Infinite-Layer Nickelates. *arXiv* [Preprint] (2021). Available from: https://arXiv.org/abs/2110.13580.
57. Xia C, Wu J, Chen Y, Chen H. Dynamical Structural Instability and a New Crystal-Electronic Structure of Infinite-Layer Nickelates. *arXiv* [Preprint] (2021). Available from: https://arXiv.org/abs/2110.12405.
58. Lu H, Rossi M, Nag A, Osada M, Li DF, Lee K, et al. Magnetic Excitations in Infinite-Layer Nickelates. *Science* (2021) 373:213–6. doi:10.1126/science.abd7726
59. Krieger G, Martinelli L, Zeng S, Chow LE, Kummer K, Arpaia R, et al. Charge and Spin Order Dichotomy in $NdNiO_2$ Driven by $SrTiO_3$ Capping Layer. *arXiv* [Preprint] (2021). Available from: https://arXiv.org/abs/2112.03341.
60. Rossi M, Osada M, Choi J, Agrestini S, Jost D, Lee Y, et al. A Broken Translational Symmetry State in an Infinite-Layer Nickelate. *arXiv* [Preprint] (2021). Available from: https://arXiv.org/abs/2112.02484.
61. Lin JQ, Villar Arribi P, Fabbris G, Botana AS, Meyers D, Miao H, et al. Strong Superexchange in a D9-δ Nickelate Revealed by Resonant Inelastic X-Ray Scattering. *Phys Rev Lett* (2021) 126:1. doi:10.1103/physrevlett.126.087001
62. Zhang GM, Yang YF, Zhang FC. Self-Doped Mott Insulator for Parent Compounds of Nickelate Superconductors. *Phys Rev B* (2020) 101:1. doi:10.1103/physrevb.101.020501
63. Wang Z, Zhang GM, Yang YF, Zhang FC. Distinct Pairing Symmetries of Superconductivity in Infinite-Layer Nickelates. *Phys Rev B* (2020) 102:1. doi:10.1103/physrevb.102.220501
64. Tsuei CC, Kirtley JR. Pairing Symmetry in Cuprate Superconductors. *Rev Mod Phys* (2000) 72:969–1016. doi:10.1103/revmodphys.72.969
65. Wu X, Jiang K, Di Sante D, Hanke W, Schnyder AP, Hu J, et al. Surface S-Wave Superconductivity for Oxide-Terminated Infinite-Layer Nickelates. *arXiv* [Preprint] (2020). Available from: https://arXiv.org/abs/2008.06009.
66. Wang BY, Li D, Goodge BH, Lee K, Osada M, Harvey SP, et al. Isotropic Pauli-Limited Superconductivity in the Infinite-Layer Nickelate Nd0.775Sr0.225NiO2. *Nat Phys* (2021) 17:473–7. doi:10.1038/s41567-020-01128-5
67. Yuan HQ, Singleton J, Balakirev FF, Baily SA, Chen GF, Luo JL, et al. Nearly Isotropic Superconductivity in (Ba,K)Fe2As2. *Nature* (2009) 457:565–8. doi:10.1038/nature07676
68. Martin C, Tillman ME, Kim H, Tanatar MA, Kim SK, Kreyssig A, et al. Nonexponential London Penetration Depth of FeAs-Based Superconducting RFeAsO(0.9)F(0.1) (R = La, Nd) Single Crystals. *Phys Rev Lett* (2009) 102:247002. doi:10.1103/PhysRevLett.102.247002
69. Chow LE, Kunniniyil Sudheesh S, Nandi P, Zeng SW, Zhang ZT, Du XM, et al. Pairing Symmetry in Infinite-Layer Nickelate Superconductor. *arXiv* [Preprint] (2022). Available from: https://arxiv.org/abs/2201.10038.
70. Harvey SP, Wang BY, Fowlie J, Osada M, Lee K, Lee Y, et al. Evidence for Nodal Superconductivity in Infinite-lLyer Nickelates. *arXiv* [Preprint] (2022). Available from: https://arxiv.org/abs/2201.12971.

Conflict of Interest: The authors declare that the research was conducted in the absence of any commercial or financial relationships that could be construed as a potential conflict of interest.

Publisher's Note: All claims expressed in this article are solely those of the authors and do not necessarily represent those of their affiliated organizations, or those of the publisher, the editors and the reviewers. Any product that may be evaluated in this article, or claim that may be made by its manufacturer, is not guaranteed or endorsed by the publisher.